Original Article
OBESITY BIOLOGY AND INTEGRATED PHYSIOLOGY

Obesity

Carbon Monoxide and Exercise Prevents Diet-Induced Obesity and Metabolic Dysregulation Without Affecting Bone

Heath G. Gasier [1,2], Tianzheng Yu[2], Joshua M. Swift[3], Corrine E. Metzger[4], Erin M. McNerny[4], Elizabeth A. Swallow[4], Claude A. Piantadosi[1,5,6], and Matthew R. Allen[4,7]

Objective: Carbon monoxide (CO) may counteract obesity and metabolic dysfunction in rodents consuming high-fat diets, but the skeletal effects are not understood. This study investigated whether low-dose inhaled CO (250 ppm) with or without moderate intensity aerobic exercise (3 h/wk) would limit diet-induced obesity and metabolic dysregulation and preserve bone health.

Methods: Obesity-resistant (OR) rats served as controls, and obesity-prone (OP) rats were randomized to sedentary, sedentary plus CO, exercise, or CO plus exercise. For 10 weeks, OP rats consumed a high-fat, high-sucrose diet, whereas OR rats consumed a low-fat control diet. Measurements included indicators of obesity and metabolism, bone turnover markers, femoral geometry and microarchitecture, bone mechanical properties, and tibial morphometry.

Results: A high-fat, high-sucrose diet led to obesity, hyperinsulinemia, and hyperleptinemia, without impacting bone. CO alone led only to a modest reduction in weight gain. Exercise attenuated weight gain and improved the metabolic profile; however, bone fragility increased. Combined CO and exercise led to body mass reduction and a metabolic state similar to control OR rats and prevented the exercise-induced increase in bone fragility.

Conclusions: CO and aerobic exercise training prevent obesity and metabolic sequelae of nutrient excess while stabilizing bone physiology.

Obesity (2020) **28**, 924-931.

Study Importance

What is already known?

- Carbon monoxide (CO) is an endogenously produced gas known to cause toxicity.
- Low-dose CO stimulates mitochondrial biogenesis in cardiac and skeletal muscle.
- Nutrient excess leads to obesity and metabolic sequelae.

What does this study add?

- Intermittent, low-dose, inhaled CO at 250 ppm has modest effects on preventing diet-induced weight gain without affecting bone.
- Intermittent, low-dose, inhaled CO at 250 ppm combined with moderate intensity aerobic exercise prevents diet-induced obesity and metabolic dysregulation and stabilizes bone physiology.

How might these results change the direction of research?

- Inhaled CO is currently being tested in a phase I trial examining feasibility and safety. The addition of low-dose inhaled CO with an exercise prescription tailored toward weight loss and/or preservation of skeletal health may allow exercise volume to be reduced, possibly increasing program compliance.

Introduction

Over the past three decades, the prevalence of obesity in the United States has increased by 21%, reaching 37.7% based on data from the National Health and Nutrition Examination Survey 2013-2014 (overall age-adjusted) (1,2). The health burden of obesity is generally associated with physical inactivity and/or excess energy intake, leading to an increased risk of developing type 2 diabetes, cardiovascular disease, and several cancers (3). Osteoporosis and fractures have traditionally not been considered important in obesity because increased body mass is positively associated with bone mineral density (spine and femoral neck) and a reduction in the relative risk of sustaining a hip fracture (4,5). When the mechanical loading effects of increased

[1] Department of Anesthesiology, Duke University School of Medicine, Durham, North Carolina, USA. Correspondence: Heath G. Gasier (heath.gasier@duke.edu) [2] Department of Military and Emergency Medicine, Uniformed Services University of the Health Sciences, Bethesda, Maryland, USA [3] Warfighter Performance, Office of Naval Research, Arlington, Virginia, USA [4] Department of Anatomy, Cell Biology and Physiology, Indiana University School of Medicine, Indianapolis, Indiana, USA [5] Department of Medicine, Duke University School of Medicine, Durham, North Carolina, USA [6] Department of Pathology, Duke University School of Medicine, Durham, North Carolina, USA [7] Roudebush Veterans Affairs Medical Center, Indianapolis, Indiana, USA.

[Correction added 2 April 2020 after original online publication. Author affiliations were originally set incorrectly.]

 Received: 18 December 2019; **Accepted:** 28 January 2020; **Published online 1 April 2020. doi:10.1002/oby.22768**

body mass are considered, however, the relationship between fat mass and bone mineral density (spine and femoral neck) becomes negative (6,7). One plausible explanation for this dichotomy is that obesity may increase fracture risk because of a reduction in bone quality, determined by structural and material properties, where the changes in bone mass (total or location) or tissue properties are insufficient to resist increased loading forces (8).

Physical activity and energy restriction are recommended for preventing the development of obesity and metabolic sequelae, but the adoption of these lifestyle modifications is challenging for most people. Alternative strategies directed at preventing the progression of overweight to obesity are, therefore, of critical importance. One approach for prevention of weight gain and the associated metabolic complications in mice is the use of carbon monoxide (CO) (9-11). Although CO is a toxic gas, possessing a greater affinity (~218 times) for hemoglobin compared with oxygen (12), it is also endogenously generated from the breakdown of heme in a reaction catalyzed by heme oxygenase (HO) (13). CO may lessen weight gain and prevent the metabolic complications associated with obesity by increasing mitochondrial capacity (11) or mitochondrial oxidative phosphorylation uncoupling (9,10), resulting in an elevated resting energy expenditure.

The effects of CO on bone are not clear, and different mechanisms of action have been reported. In the ovariectomized mouse, CO-releasing molecule (CORM)-2 administered daily for 8 weeks attenuated bone loss and reduced indices of bone resorption and plasma levels of H_2O_2 (14). In parallel *in vitro* experiments using mouse bone marrow cells, the authors reported that CORM-2 inhibited osteoclastogenesis by reducing receptor activator of nuclear factor-κB ligand (RANKL) and oxidant production (14). In addition, CO was reported to increase proliferation of bone marrow mesenchymal stem cells and their differentiation into osteoblasts versus adipocytes (15). Indeed, diet-induced obesity was shown to not only induce osteoclastogenesis, in part through RANKL activation, but also to increase bone marrow adipocyte expansion in mice and rats (16). Beneficial properties of CO may, therefore, extend to bone in obesity by suppressing osteoclastogenesis and/or stimulation of bone marrow mesenchymal cells into osteoblasts versus adipocytes.

Because the antiobesity effectiveness of CO has not been compared with exercise, our primary research objective was to determine whether intermittent, low-dose, inhaled CO with and without aerobic exercise impacts weight gain and the metabolic sequelae of diet-induced obesity and whether the effects are extended to bone. We hypothesized CO would prevent adiposity and metabolic dysregulation and preserve bone geometry, microarchitecture, and mechanical properties with higher effectiveness when combined with exercise.

Methods

Animals and experimental design

Obesity-prone (OP) and obesity-resistant (OR) male rats (Charles River, Germantown, Maryland) aged 8 to 9 weeks old were used in accordance with and with approval of the Uniformed Services University of the Health Sciences Institutional Animal Care and Use Committee. Animals were housed in pairs in a climate-controlled animal facility with a 12:12-hour light-dark cycle (light on at 6:00 PM and lights off at 6:00 AM). OP rats develop an obese phenotype with high-fat feeding without interference from gene manipulation, and OR rats maintain a lean phenotype throughout their life-span. In order to minimize prestudy weight differences between the four OP groups, rats were assigned by body mass to serve either as sedentary controls (OP, $n=14$), sedentary with CO exposure (OP+CO, $n=14$), exercise (OP+EX, $n=11$), or CO with exercise (OP+COEX, $n=10$). Upon arrival from Charles River, all rats received a standard chow ad libitum and had free access to water during habituation to involuntary treadmill running, CO exposures, and glucose tolerance testing (~2 weeks). Thereafter, OR rats were switched to a low-fat control diet containing 3.6 kcal/g, 68% kilocalories from carbohydrate (sucrose 120 g/kg), 19% kilocalories from protein, and 13% kilocalories from fat (TD.08485; Teklad Custom, Harlan Laboratories, Madison, Wisconsin), and OP rats were switched to a high-fat, high-sucrose diet that contained 4.5 kcal/g, 43% kilocalories from carbohydrate (sucrose 341 g/kg), 15% kilocalories from protein, and 42% kilocalories from fat (62% saturated fat) (TD.88137). Rats received the research diets ad libitum and had free access to water, and food consumption was recorded biweekly throughout the 10-week protocol. Body mass was determined weekly. Glucose tolerance testing was completed within 48 hours of completing the 10-week protocol.

Exercise protocol

OP rats randomized to exercise training (OP+EX and OP+COEX) were habituated to a three-lane rodent treadmill with shock stimulus (Exer 3/6; Columbus Instruments, Columbus, Ohio) over 10 sessions (2 weeks), starting at 10 m/min for 5 minutes and increasing up to a maximum of 22 m/min over 10 minutes at a grade of 10°. The shock current and rate were ≤0.5 mA and 1 Hz over 5 seconds, respectively. Following habituation, the animals performed 3 h/wk (alternating between 3×1 hour and 4×45 minutes) of exercise training, starting at 20 m/min and increasing by 1 m/min each week to a maximum of 25 m/min at a grade of 10°. The animals received chocolate (Hershey's, Hershey, Pennsylvania) after each training session for positive reinforcement.

CO exposure

OP+CO and OP+COEX rats received five 1-hour CO treatments prior to switching the animals to the high-fat and high-sucrose diet and then biweekly throughout the 10-week protocol. During the study, the CO treatments were interspersed by a minimum of 48 hours and always administered after exercise training (OP+COEX rats). CO (Roberts Oxygen Company, Inc., Rockville, Maryland) was delivered to the animals placed in a flow-through induction box. The flow rate was adjusted to maintain a CO level of 250 ppm, verified by a CO meter (GasBadge Pro Gas Detector; Industrial Scientific, Pittsburgh, Pennsylvania) housed within the box. In a different group of OR rats ($n=18$) ranging in weight from 405 to 456 g, pre-, post-, and 5-hour post-CO venous blood samples were collected from the lateral saphenous vein, placed in lithium heparin blood collection tubes, sealed, and shipped overnight to Duke University Center for Hyperbaric Medicine and Environmental Physiology, Durham, North Carolina, for the determination of carboxyhemoglobin (COHb) using an automated CO analyzer (IL 682 CO-Oximeter; Instrumentation Laboratory, Bedford, Massachusetts).

Glucose tolerance testing

Before and after the 10-week protocol and after a 12-hour fast, rats received an intraperitoneal injection of glucose (2 g/kg body weight). Blood glucose was monitored at 0, 15, 30, 60, 90, and 120 minutes following glucose delivery using a portable glucometer (OneTouch Ultra 2; LifeScan, Inc., Wayne, Pennsylvania).

Plasma measurements

At the end of the study and following an overnight fast, animals were anesthetized with isoflurane, and blood was collected via the left ventricle in K_2EDTA vacutainers; it was separated by centrifugation (3,800*g* for 15 minutes at 4°C). Plasma was aliquoted into 2-mL cryogenic tubes and frozen at −80°C until analysis. Commercially available enzyme-linked immunosorbent assay kits and an iMark Microplate Absorbance Reader (Bio-Rad, Hercules, California) were used to determine plasma insulin (ALPCO, Salem, New Hampshire), insulinlike growth factor 1 (IGF-1), C-reactive protein (CRP) (Thermo Fisher Scientific, Frederick, Maryland), leptin (Novex Life Technologies, Frederick, Maryland), adiponectin (EMD Millipore, Billerica, Massachusetts), and N-terminal propeptide of type I procollagen (PINP), C-terminal telopeptide of type I collagen, osteocalcin, and osteoclast-derived tartate-resistant acid phosphatase isoform 5b (Immunodiagnostic Systems, Gaithersburg, Maryland).

Adipocyte staining and quantification

Epididymal fat pads (white adipose tissue) were excised after euthanasia and freshly weighed. A section was fixed in 10% formalin, paraffin embedded, cut into 5-μm slices, and stained with hematoxylin and eosin. Slides were imaged with a Zeiss Axio Scan.Z1 (Carl Zeiss Microscopy, LLC, White Plains, New York) at 20× magnification in bright field mode. Total number and area were determined from four to six different regions per animal using ImageJ (National Institutes of Health, Bethesda, Maryland).

Microcomputed tomography

The left femurs were harvested, cleaned of tissue, wrapped in phosphate-buffered saline-soaked gauze, placed in 5-mL conical scintillation vials, and stored at 4°C prior to shipping to the Indiana University School of Medicine, Indianapolis, Indiana. Whole femora were scanned using an 18-μm isotropic voxel size on a SkyScan 1176 microcomputed tomography (CT) system (Bruker, Billerica, Massachusetts). Scans were reconstructed and rotated using manufacturer-supplied software. Cortical bone area, cortical cross-sectional thickness, and mean polar moment of inertia were determined at the mid-diaphysis (one section located at 50% total length). Trabecular bone volume/tissue volume (BV/TV), trabecular number (Tb.N), and trabecular thickness were determined at the distal femur metaphysis (1-mm region located ~0.5 mm proximal to the growth plate). Cortical and trabecular bone scans and analyses were conducted as previously described (17,18).

Mechanical testing

Four-point bending tests were completed with the same femora that were used for micro-CT scans as described (19,20). In brief, bones were placed anterior side down on fixtures that were 18 mm apart. The upper fixture points were positioned, centered at midpoint of the bone, and separated by 6 mm. Bones were displaced at a rate of 2 mm/min until fracture. Force and displacement data were collected at 15 Hz. Using a custom MATLAB program, data were plotted and analyzed to determine the ultimate load, stiffness, and energy to failure. Using geometry from micro-CT, material-level properties were calculated using beam-bending equations for estimating ultimate stress, modulus, and toughness.

Histomorphometry

Nine and two days prior to euthanasia, rats were injected subcutaneously in the midscapular region with calcein (25 mg/kg body mass), pH 7.0. Following euthanasia, tibiae were harvested, cleaned of tissue, and placed in 10% formalin for 48 hours before changing to 70% ethanol. The bones were kept at 4°C and shipped to the Indiana University School of Medicine. Tibiae were subjected to serial dehydration and embedded in methyl methacrylate. Semithin sections (4 μm) were cut using a microtome, fixed to slides, and cover-slipped unstained. Trabecular bone surfaces were measured for single, double, and no label; regions with double label were further analyzed to determine the distance between labels. The mineral apposition rate (MAR), mineralizing surface/bone surface (MS/BS), and bone formation rate (BFR) were calculated as follows: MAR = (interlabel distance / 7 [number of days between calcein label administration]); MS/BS = ([1/2 single label surface + double label surface] / total surface × 100); and bone formation rate = (MAR × MS/BS). All measures, calculations, and nomenclature used here were in accordance with the recommendations provided by the American Society for Bone and Mineral Research (21).

Statistical analysis

Data were analyzed using SigmaPlot 14.0 (Systat Software, Inc., San Jose, California) and SPSS Statistics 26 (IBM Corp., Armonk, New York). Before experimentation, OR and OP baseline data were compared using a *t* test. A one-way ANOVA was used to compare experimental mean group differences, and when a significant main effect was observed, post hoc testing was completed with a Bonferroni *t* test. For measures in which the sample size and variances were unequal, a one-way ANOVA with Welch test followed by Games-Howell post hoc test (when appropriate) was performed. Values of $P<0.05$ were considered statistically significant.

Results

Changes in venous blood COHb following CO exposures

A 1-hour exposure to CO at 250 ppm increased COHb from 0.14% (SE 0.08%) to 18.11% (SE 1.23%) ($P<0.001$), dropping to 1.13% (SE 0.05%) when measured 5 hours later (Figure 1). The COHb levels after a 1-hour CO exposure (250 ppm) were consistent with previously reported values (22).

Effects of 10-week diet-induced obesity model on adiposity and hormonal changes

Prior to study initiation, OP animals weighed significantly more (mean [SE] 389 [4] g vs. 313 [5] g, $P<0.001$) and had higher fasting blood glucose (104 [2] mg/dL vs. 97 [2] mg/dL, $P=0.014$) and glucose area under the curve (19,030 [505] vs. 16,354 [279], $P<0.001$) compared with OR rats. After the 10-week diet-induced obesity protocol, body weights were as follows: mean (SE), OR, 433 (7) g; OP, 701 (11) g; OP+CO, 665 (7) g; OP+EX, 560 (16) g; and OP+COEX, 519 (12) g. Mean (SE) daily energy intake among OR rats was calculated to be 74 (1) kcal, whereas OP and OP+CO animals consumed 129 (4) kcal/d and 128 (3) kcal/d, respectively ($P<0.001$) (Figure 2A). In contrast to OP sedentary rats, OP+EX and OP+COEX groups consumed significantly less food, 105 (2) kcal/d and 104 (4) kcal/d, respectively ($P<0.001$). Surprisingly, the similar energy consumption between OP and OP+CO rats and OP+EX and OP+COEX rats led to statistically different weight gain among the groups ($P<0.001$) (Figure 2B). OP+CO rats tended to gain less weight than OP rats (12%, $P=0.075$), and OP+COEX rats gained significantly less (36%) weight than EX rats

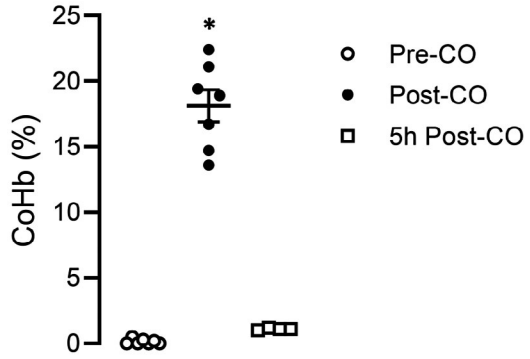

Figure 1 Percentage of carboxyhemoglobin (COHb) in venous blood. Rats were placed in an induction box and exposed to 250 ppm of CO for 1 hour, consistent with the experimental dosage. Circles and lines represent individual data points with means (SE). Pre- and post-CO, $n=7$; 5-hour post-CO, $n=4$. *Significantly different from pre-CO, $P<0.001$.

($P<0.001$), with no observed differences between OP+COEX and OR rats. Epididymal fat pad weight and white adipocyte size were statistically greater in OP and OP+CO rats ($P<0.05$), and exercise prevented this increase (Figure 2C-2E).

Obesity is known to alter glucose and insulin homeostasis and leptin signaling, as found in OP and OP+CO rats (Table 1). Although obesity led to an increase in plasma adiponectin levels, the leptin:adiponectin ratio was ~2.2- and 2.0-fold greater compared with OR rats, respectively. Exercise effectively prevented the metabolic sequelae of high-fat, high-sucrose feeding, and the combination of CO and exercise further attenuated the rise in insulin and prevented the reduction in adiponectin levels compared with OP animals. IGF-1 levels were significantly higher in OP (+74%), OP+CO (+57%), and OP+EX (+54%) groups compared with OR rats. CRP levels did not differ among the groups.

Plasma bone turnover biomarkers and bone histomorphometry

Of the bone formation markers examined, PINP was 71% greater in OP+COEX rats compared with OR rats, while a borderline increase ($P=0.07$-0.09) was observed for PINP in OP, OP+CO, and OP+EX groups (Table 2). For bone resorption, a trend was observed for lower osteoclast-derived tartate-resistant acid phosphatase isoform 5b levels in OP+EX rats ($P=0.09$). No measures of dynamic bone formation activity determined in the proximal tibia trabecular bone differed among the groups (Table 3).

Bone architecture/geometry

The femoral cortical area (+10%-20%) and cross-sectional moment of inertia (+45%-49%) were higher in OP, OP+CO, and OP+EX groups compared with OR rats, while cortical thickness did not differ among groups (Figure 3A-3C). Although the higher cortical area observed in the OP group was attenuated in OP+COEX animals, cortical geometric properties were similar between OR and OP+COEX rats. The microarchitecture of cancellous bone was unaffected by diet-induced obesity (Figure 3D-3F). BV/TV was 62% higher in OP+EX rats, and there was a trend for an increase in OP+COEX rats compared with OR rats ($P = 0.09$). Exercise with and without CO resulted in a 30% increase in Tb.N when compared with OR rats. Trabecular thickness did not significantly differ between groups.

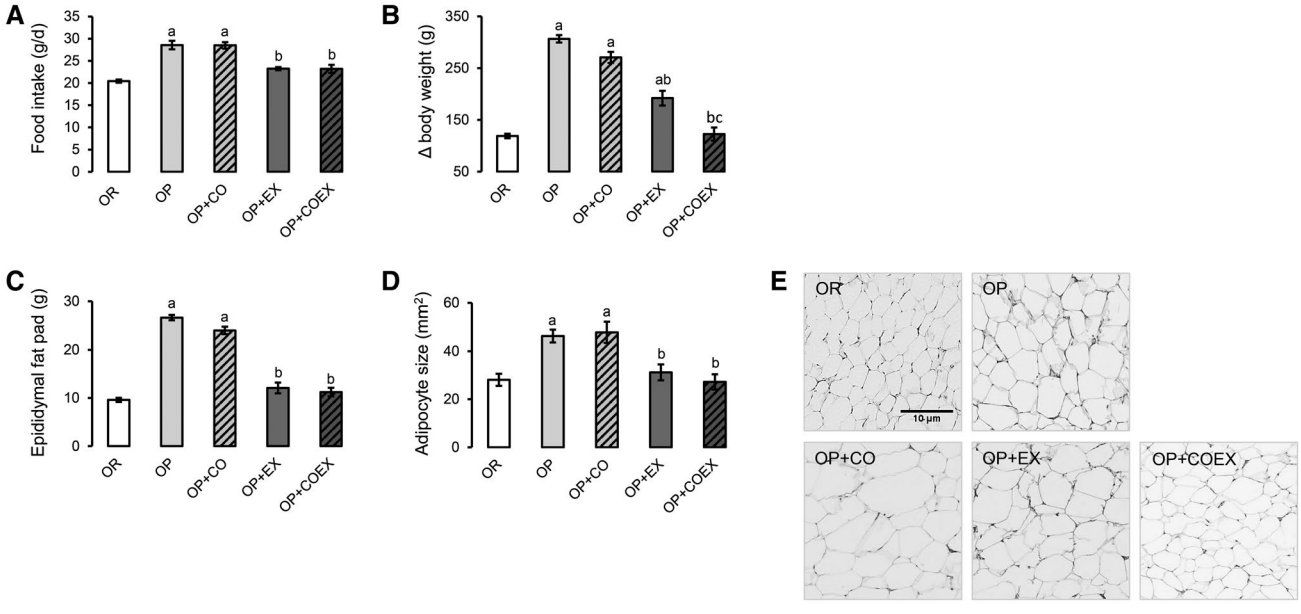

Figure 2 Food intake and adiposity. (**A**) Mean daily food consumption, (**B**) changes in body weight, (**C**) epididymal fat pad weight, (**D**) and adipocyte size determined from hematoxylin and eosin (H&E) stained sections. For quantification, four to six areas per animal were used. (**E**) Representative H&E images (20× magnification). Values are presented as means (SE); $n=9$ to 15 per group. Compared with [a]OR, [b]OP, and [c]OP-EX groups, $P<0.05$.

TABLE 1 Blood glucose and plasma biomarkers

	OR	OP	OP+CO	OP+EX	OP+COEX	*P* value
n	14	15	14	11	10	
Glucose, mg/dL	103 (4)	110 (3)	117 (3)[a]	100 (3)	103 (3)	0.003
Glucose, AUC*	18,279 (604)	22,735 (1,397)	21,700 (1,413)	20,177 (949)	20,639 (1,141)	0.035
Insulin, μIU/mL	16.1 (2.3)	47.8 (8.4)[a]	35.5 (3.9)	27.0 (7.2)	21.6 (4.5)[b]	0.004
HOMA-IR	4.2 (0.7)	11.6 (1.5)[a]	10.4 (1.2)[a]	6.7 (1.7)	5.6 (1.2)[b]	0.001
Leptin, ng/mL	2.5 (0.3)	9.1 (0.6)[a]	8.3 (0.6)[a]	3.7 (0.5)[b]	2.0 (0.4)[b]	0.001
Adiponectin, mg/mL*	12.2 (1.1)	19.2 (1.3)[a]	19.0 (1.5)[a]	11.4 (0.6)[b]	14.1 (1.5)	0.000
Leptin/adiponectin	0.24 (.04)	0.51 (0.04)[a]	0.47 (0.4)[a]	0.33 (0.04)[b]	0.16 (0.02)[b]	0.001
IGF-1, ng/mL	752 (46)	1,306 (55)[a]	1,180 (87)[a]	1,155 (63)[a]	917 (90)[b,c]	0.001
C-reactive protein, μg/mL*	460 (49)	456 (18)	507 (45)	406 (37)	443 (24)	0.567

Values presented as means (SE).
Glucose tolerance test performed on final day of 10-week experiment to determine fasting glucose and area under the curve (AUC). Hormones and C-reactive protein determined from blood collected at time of euthanasia.
[a]Compared with OR group.
[b]Compared with OP group.
[c]Compared with OP+EX group.
*Indicates data analyzed with one-way ANOVA with Welch test because of heterogeneity in variances.
HOMA-IR, homeostatic model of insulin resistance; IGF-1, insulinlike growth factor 1.

TABLE 2 Plasma bone formation and resorption markers

	OR	OP	OP+CO	OP+EX	OP+COEX	*P* value
n	10-12	10-12	10-14	8-10	8-10	
PINP, mg/mL	18 (1)	27 (3)	37 (6)	31 (4)	30 (2)[a]	0.001*
Osteocalcin, ng/mL	409 (31)	334 (51)	369 (42)	396 (52)	505 (90)	0.290
CTX-I, ng/mL	20 (2)	15 (1)	17 (1)	16 (1)	16 (1)	0.189
TRAcP 5b, U/L	5.8 (0.9)	4.7 (0.7)	5.3 (0.6)	3.1 (0.3)	3.3 (0.5)	0.029

Values presented as means (SE). Bone markers determined from blood collected at time of euthanasia.
[a]Compared with OR group.
*Indicates data analyzed with one-way ANOVA with Welch test because of heterogeneity in variances.
CTX-I, C-terminal telopeptide of type I collagen; PINP, type I procollagen N-terminal propeptide; TRAcP, tartate-resistant acid phosphatase isoform 5b.

Mechanical properties

Diet-induced obesity led to higher bone stiffness in OP (+27%) and OP+CO (+18%) rats, while exercise alone attenuated this effect (Figure 4A). Ultimate force was similar between groups (Figure 4B), while the work to fracture was reduced in exercised rats compared with OP rats (Figure 4C). In accounting for bone size (material properties), a significant main effect was observed for modulus, ultimate stress, and toughness; however, the only significant difference by post hoc testing was toughness, which was ~2.3-fold lower in OP+EX rats compared with OR rats (Figure 4D-4F).

Discussion

More than a decade ago, the antiobesity effects of heme oxygenase 1 induction were first reported (23). Therapeutic investigations have since explored the efficacy of CO in mouse models of obesity (9-11). These studies have all reported a short-term reduction in weight gain and an improvement in metabolic profiles. It is unknown whether the CO effects are similar to exercise or whether they extend to the musculoskeletal system. Here, we explored the potential of intermittent, low-dose, inhaled CO, independently and combined with load-bearing aerobic exercise, to prevent adiposity, early-phase metabolic dysregulation, and changes in bone health in skeletally mature rats. Our new findings indicate the following: First, while OP rats developed an obesity phenotype that was associated with hyperinsulinemia, elevated homeostatic model of insulin resistance, and hyperleptinemia, cortical bone morphometry and mechanical properties as well as cancellous bone microarchitecture and cell activity were not negatively affected. Second, biweekly 1-hour CO exposures at 250 ppm provided a modest reduction in weight gain without affecting bone. And third, CO combined with exercise led to anthropometric changes, a metabolic profile and bone properties that were similar to those of OR rats.

To explain, the 10-week diet-induced obesity intervention led to expansion of white adipose tissue, hyperinsulinemia, and insulin resistance, evidenced by an increase in the homeostatic model of insulin resistance and plasma leptin to adiponectin ratio (24). The anorexigenic hormone leptin, which was increased in OP rats by ~3.6-fold over OR rats, directly stimulates the proliferation and differentiation of bone marrow mesenchymal stem cells into osteoblasts (peripheral mechanism) or indirectly induces osteoclastogenesis via

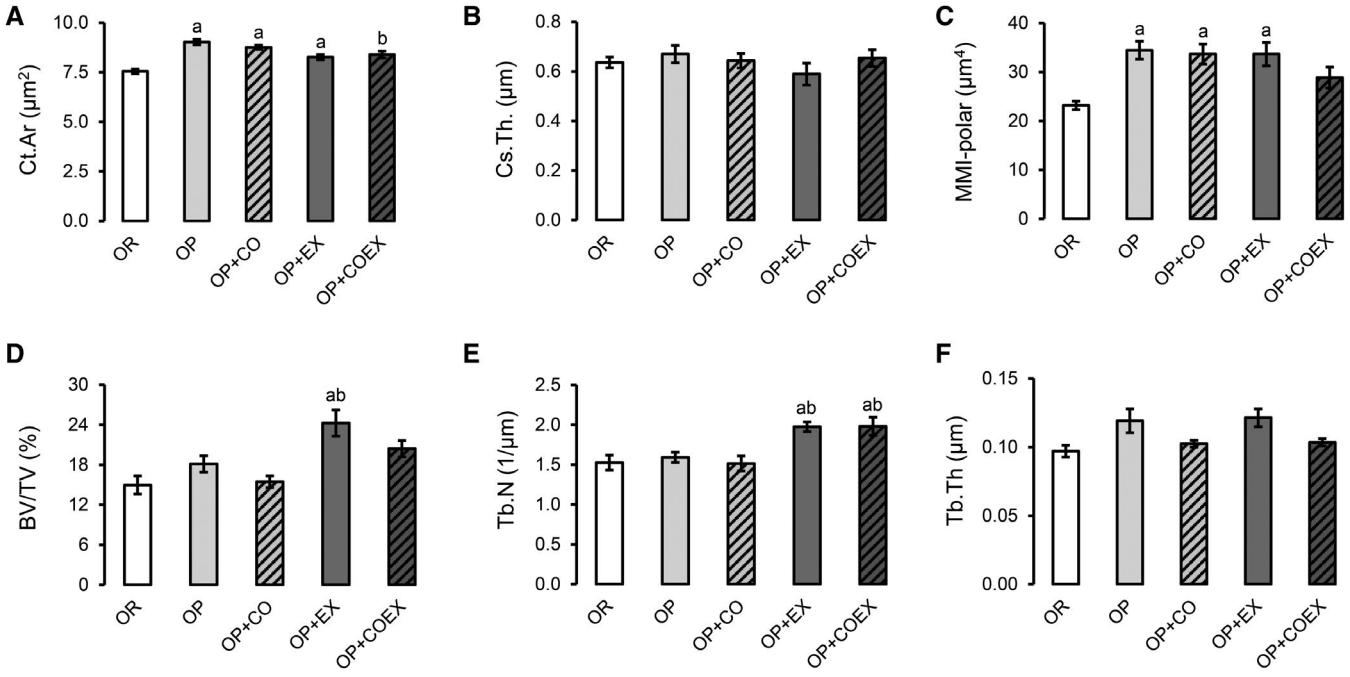

Figure 3 Femur cortical geometric properties and cancellous microarchitecture determined by micro-CT. Cortical properties were determined at the mid-diaphysis. (**A**) Cortical area (Ct.Ar), (**B**) cortical cross-sectional thickness (Cs.Th), and (**C**) mean polar moment of inertia (MMI-polar). Cancellous properties were determined at the proximal metaphysis. (**D**) Bone volume (BV/TV), (**E**) trabecular number (Tb.N), and (**F**) trabecular thickness (Tb.Th). Values are presented as means (SE); $n = 10$-15 per group. Compared with [a]OR and [b]OP rats, $P < 0.05$.

TABLE 3 Dynamic histomorphometry analyses determined at proximal tibia metaphysis

	OR	OP	OP+CO	OP+EX	OP+COEX	*P* value
n	9-10	9-10	9	10	10	
MAR, μm/d	0.92 (0.09)	0.82 (0.06)	0.87 (0.04)	0.77 (0.06)	0.91 (0.07)	0.461
MS/BS, %	19.9 (1.8)	18.2 (0.8)	17.1 (1.1)	16.7 (1.6)	20.2 (1.3)	0.257
BFR, μm³/μm²/d	72.4 (12.3)	53.7 (5.5)	54.5 (4.9)	48.4 (7.6)	69.6 (9.4)	0.189

Values presented as means (SE).
BFR, bone formation rate; MAR, mineral apposition rate; MS/BS, mineralizing surface.

increased sympathetic nerve activity (central mechanism) (25). In contrast to typical obesity (26), adiponectin levels were 57% higher in OP rats compared with OR rats. Adiponectin is known to stimulate insulin secretion, glucose uptake, lipid oxidation, and anti-inflammatory effects (27,28). Also, adiponectin was shown to inhibit osteoclastogenesis *in vitro* by suppressing the RANKL and p38 signaling pathways (29). Because plasma adiponectin and osteocalcin, which is a modulator of insulin secretion and glucose homeostasis (30), did not decrease and CRP did not increase, glucose intolerance and chronic systemic inflammation did not yet develop. These findings suggest that obesity progression was in the early phase.

Our model of diet-induced obesity did not compromise femoral cortical or cancellous bone. Generally, in mice (31-33) and rats (34-36), cancellous but not cortical bone is affected by diet-induced obesity. Here, we found increased cortical bone area, mean polar moment of inertia and stiffness, and plasma IGF-1, suggesting femur cortical bone was adapting to mechanical loading induced by the increasing body mass. The lack of differences in femur cancellous morphometry and tibial bone formation between OR and OP rats implies that the cortical bone is being targeted for adaptation to increased body weight. The differences reported herein and from the references are perhaps due to differences in the species and strain, gender and age, and diet composition and the duration of the dietary protocol. In any event, our data suggest that in the early phase of obesity when glucose intolerance and chronic systemic inflammation were not yet apparent, femoral bone was not compromised.

Contrary to our hypothesis, CO alone did not prevent diet-induced obesity and the metabolic sequelae. The CO treatment profile consisted of five 1-hour treatments at 250 ppm before changing the diet to high-fat and high-sucrose, an exposure similar to that being tested for safety in a phase I clinical trial (37), and biweekly during the 10-week experiment using the same dosage interspersed by 48 hours. The rationale for treating the rats intermittently versus daily was to avoid toxicity, including

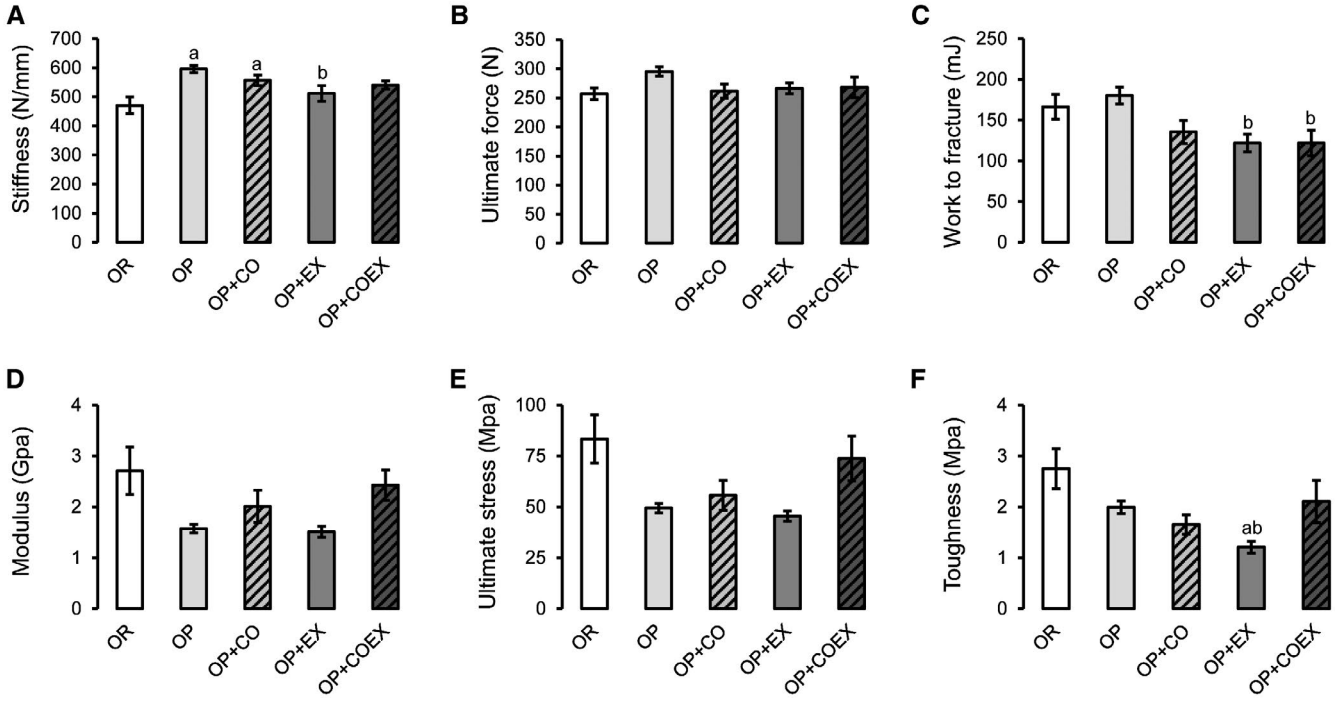

Figure 4 Biomechanical properties of the femoral diaphysis determined by four-point bending tests. Structural properties included (**A**) stiffness, (**B**) ultimate force, and (**C**) work to fracture. Material properties included (**A**) modulus, (**B**) ultimate stress, (**C**) and toughness and were analyzed using a one-way ANOVA with Welch test because of heterogeneity in variances. Values are presented as means (SE); $n = 10$-15 per group. Compared with [a]OR and [b]OP rats, $P < 0.05$.

reduced food intake, and maintaining stable redox balance. Obesity and CO stimulate cellular oxidant production (38,39). For instance, Zheng et al. (40) explored the daily use of CO (250 ppm for 2 hours) in mice over the final 10 weeks of a 16-week diet-induced obesity experiment and reported lower weight gain, body fat, and serum leptin and less endoplasmic reticulum stress; however, the CO animals in the high-fat diet group consumed significantly less food, consistent with hypoxia. In this study, food intake was similar between OP and OP+CO rats and OP+EX and OP+COEX rats. We thus avoided sustained hypoxia and, perhaps, excessive oxidant production, but only a weak antiobesity potential of CO was apparent, i.e., the final body mass was only 5% lower in OP+CO rats compared with OP rats and the metabolic profiles were similar. The antiobesity effectiveness of CO may have been greater had we used CORMs (10,41) because CORMs allow for cellular targeting and controlled release of CO (42). However, our CO protocol differed from others (40,41); comparisons of the antiobesity effectiveness of inhaled CO versus CORMs have not been reported, and conclusions remain speculative.

Our protocol of treadmill running reduced diet-induced weight gain by 20% and prevented hyperinsulinemia and hyperleptinemia. In addition to the favorable cortical morphometric responses to obesity, we found increased trabecular BV/TV and Tb.N, implying improved cancellous femur structure, consistent with an earlier study (36). Exercise did attenuate obesity-induced increases in stiffness and work to fracture, but the measurements were similar to OR rats. Taking bone size into account, however, the tissue properties trended downward compared with OR rats, becoming significant only for toughness, a measure of fracture resistance. This may imply that the cortical geometric adaptations were insufficient to sustain the repetitive forces imposed by running and increasing body mass, i.e., OP+EX rats still were 61% heavier than OR rats at the end of the study. This was surprising because exercise is generally recognized to improve bone toughness as long as the intensity is not high enough to produce damage. Our rats performed only 3 hours over three to four sessions per week at a moderate intensity, an appropriate training volume shown to improve skeletal health in rats (43).

CO plus exercise led to weight gain and a metabolic profile that closely mirrored OR rats despite similarities in food intake and exercise volume between the OP+COEX and OP+EX groups. This suggests that whole body energy expenditure increased and may be attributed partly to an additive effect of low-dose inhaled CO and moderate exercise on mitochondrial bioenergetics, dynamics, and quality control (44,45). For the bone, BV/TV (trend) and Tb.N were similar to OP+EX rats, indicating running and not body mass led to better cancellous bone structure. In contrast to OP+EX rats, cortical bone geometry and material properties did not differ from OR rats. Therefore, CO prevented the increase in bone fragility that was observed with exercise alone. The disparity between OP+EX and OP+COEX rats is not easily attributed to hormonal responses because leptin, adiponectin, and IGF-1 levels were similar. CO does suppress osteoclastogenesis and stimulates osteoblastogenesis (14,15), yet because obesity alone did not result in bone loss, this is questionable. Instead and more plausibly, the further reduction in body mass caused by CO plus aerobic exercise was responsible for the differences in femoral material properties between OP+EX and OP+COEX rats.

In summary, 10 weeks of diet-induced obesity led to adiposity, hyperinsulinemia, and hyperleptinemia in rats, although the increase in

adiponectin and normal CRP indicate glucose intolerance and systemic chronic inflammation were still absent. Given the measured IGF-1, femur cortical and cancellous bone responded favorably or were unaltered by obesity, respectively. Also, while CO administration has been successful in reducing weight gain in mice, low-dose CO led to only a modest reduction in weight gain. Higher doses or more frequent CO treatments in rats require a control for hypoxia and may not avoid direct toxicity. The combination of CO and exercise also prevented increased bone fragility observed with exercise alone. These data indicate more research is needed on combination CO and exercise protocols to prevent or treat obesity and metabolic disorders that affect skeletal health.**O**

Funding agencies: This research was supported by the Uniformed Services University of the Health Sciences (USUHS) Office of Research and the Defense Health Program (0130-16-0003-00001 to HG). The views expressed are those of the authors and do not reflect the official position of the USUHS, United States Navy, or United States Department of Defense.

Disclosure: The authors declared no conflict of interest.

References

1. An R, Xiang X. Age-period-cohort analyses of obesity prevalence in US adults. *Public Health* 2016;141:163-169.
2. Flegal KM, Kruszon-Moran D, Carroll MD, Fryar CD, Ogden CL. Trends in obesity among adults in the United States, 2005 to 2014. *JAMA* 2016;315:2284-2291.
3. Wang YC, McPherson K, Marsh T, Gortmaker SL, Brown M. Health and economic burden of the projected obesity trends in the USA and the UK. *Lancet* 2011;378:815-825.
4. De Laet C, Kanis JA, Oden A, et al. Body mass index as a predictor of fracture risk: a meta-analysis. *Osteoporos Int* 2005;16:1330-1338.
5. Yang S, Shen X. Association and relative importance of multiple obesity measures with bone mineral density: the National Health and Nutrition Examination Survey 2005-2006. *Arch Osteoporos* 2015;10:14. doi:10.1007/s11657-015-0219-2
6. Zhang P, Peterson M, Su GL, Wang SC. Visceral adiposity is negatively associated with bone density and muscle attenuation. *Am J Clin Nutr* 2015;101:337-343.
7. Zhao LJ, Liu YJ, Liu PY, Hamilton J, Recker RR, Deng HW. Relationship of obesity with osteoporosis. *J Clin Endocrinol Metab* 2007;92:1640-1646.
8. Turner CH. Biomechanics of bone: determinants of skeletal fragility and bone quality. *Osteoporos Int* 2002;13:97-104.
9. Braud L, Pini M, Muchova L, et al. Carbon monoxide-induced metabolic switch in adipocytes improves insulin resistance in obese mice. *JCI Insight* 2018;3:e123485. doi:10.1172/jci.insight.123485
10. Hosick PA, AlAmodi AA, Storm MV, et al. Chronic carbon monoxide treatment attenuates development of obesity and remodels adipocytes in mice fed a high-fat diet. *Int J Obes (Lond)* 2014;38:132-139.
11. Upadhyay KK, Jadeja RN, Vyas HS, et al. Carbon monoxide releasing molecule-A1 improves nonalcoholic steatohepatitis via Nrf2 activation mediated improvement in oxidative stress and mitochondrial function. *Redox Biol* 2020;28:101314. doi:10.1016/j.redox.2019.101314
12. Rodkey FL, O'Neal JD, Collison HA. Oxygen and carbon monoxide equilibria of human adult hemoglobin at atmospheric and elevated pressure. *Blood* 1969;33:57-65.
13. Tenhunen R, Marver HS, Schmid R. Microsomal heme oxygenase. Characterization of the enzyme. *J Biol Chem* 1969;244:6388-6394.
14. Van Phan T, Sul OJ, Ke K, et al. Carbon monoxide protects against ovariectomy-induced bone loss by inhibiting osteoclastogenesis. *Biochem Pharmacol* 2013;85:1145-1152.
15. Li J, Song L, Hou M, Wang P, Wei L, Song H. Carbon monoxide releasing molecule3 promotes the osteogenic differentiation of rat bone marrow mesenchymal stem cells by releasing carbon monoxide. *Int J Mol Med* 2018;41:2297-2305.
16. Shu L, Beier E, Sheu T, et al. High-fat diet causes bone loss in young mice by promoting osteoclastogenesis through alteration of the bone marrow environment. *Calcif Tissue Int* 2015;96:313-323.
17. Lima F, Swift JM, Greene ES, et al. Exposure to low-dose x-ray radiation alters bone progenitor cells and bone microarchitecture. *Radiat Res* 2017;188:433-442.
18. Moe SM, Chen NX, Newman CL, et al. A comparison of calcium to zoledronic acid for improvement of cortical bone in an animal model of CKD. *J Bone Miner Res* 2014;29:902-910.
19. Berman AG, Clauser CA, Wunderlin C, Hammond MA, Wallace JM. Structural and mechanical improvements to bone are strain dependent with axial compression of the tibia in female C57BL/6 mice. *PLoS One* 2015;10:e0130504. doi:10.1371/journal.pone.0130504
20. Vesper EO, Hammond MA, Allen MR, Wallace JM. Even with rehydration, preservation in ethanol influences the mechanical properties of bone and how bone responds to experimental manipulation. *Bone* 2017;97:49-53.
21. Dempster DW, Compston JE, Drezner MK, et al. Standardized nomenclature, symbols, and units for bone histomorphometry: a 2012 update of the report of the ASBMR Histomorphometry Nomenclature Committee. *J Bone Miner Res* 2013;28:2-17.
22. Benignus VA, Annau Z. Carboxyhemoglobin formation due to carbon monoxide exposure in rats. *Toxicol Appl Pharmacol* 1994;128:151-157.
23. Li M, Kim DH, Tsenovoy PL, et al. Treatment of obese diabetic mice with a heme oxygenase inducer reduces visceral and subcutaneous adiposity, increases adiponectin levels, and improves insulin sensitivity and glucose tolerance. *Diabetes* 2008;57:1526-1535.
24. Nguyen PA, Heggermont WA, Vanhaverbeke M, et al. Leptin-adiponectin ratio in pre-diabetic patients undergoing percutaneous coronary intervention. *Acta Cardiol* 2015;70:640-646.
25. Chen XX, Yang T. Roles of leptin in bone metabolism and bone diseases. *J Bone Miner Metab* 2015;33:474-485.
26. Saltevo J, Laakso M, Jokelainen J, Keinanen-Kiukaanniemi S, Kumpusalo E, Vanhala M. Levels of adiponectin, C-reactive protein and interleukin-1 receptor antagonist are associated with insulin sensitivity: a population-based study. *Diabetes Metab Res Rev* 2008;24:378-383.
27. Patane G, Caporarello N, Marchetti P, et al. Adiponectin increases glucose-induced insulin secretion through the activation of lipid oxidation. *Acta Diabetol* 2013;50:851-857.
28. Scherer PE. The multifaceted roles of adipose tissue-therapeutic targets for diabetes and beyond: the 2015 banting lecture. *Diabetes* 2016;65:1452-1461.
29. Chen G, Huang L, Wu X, et al. Adiponectin inhibits osteoclastogenesis by suppressing NF-kappaB and p38 signaling pathways. *Biochem Biophys Res Commun* 2018;503:2075-2082.
30. Lee NK, Sowa H, Hinoi E, et al. Endocrine regulation of energy metabolism by the skeleton. *Cell* 2007;130:456-469.
31. Cao JJ, Gregoire BR, Gao H. High-fat diet decreases cancellous bone mass but has no effect on cortical bone mass in the tibia in mice. *Bone* 2009;44:1097-1104.
32. Cao JJ, Sun L, Gao H. Diet-induced obesity alters bone remodeling leading to decreased femoral trabecular bone mass in mice. *Ann N Y Acad Sci* 2010;1192:292-297.
33. Picke AK, Sylow L, Moller LLV, et al. Differential effects of high-fat diet and exercise training on bone and energy metabolism. *Bone* 2018;116:120-134.
34. Cao JJ, Picklo MJ Sr. Involuntary wheel running improves but does not fully reverse the deterioration of bone structure of obese rats despite decreasing adiposity. *Calcif Tissue Int* 2015;97:145-155.
35. Hinton PS, Shankar K, Eaton LM, Rector RS. Obesity-related changes in bone structural and material properties in hyperphagic OLETF rats and protection by voluntary wheel running. *Metabolism* 2015;64:905-916.
36. Ortinau LC, Linden MA, Dirkes RK, Rector RS, Hinton PS. Exercise initiated after the onset of insulin resistance improves trabecular microarchitecture and cortical bone biomechanics of the tibia in hyperphagic Otsuka Long Evans Tokushima Fatty rats. *Bone* 2017;103:188-199.
37. Fredenburgh LE, Perrella MA, Barragan-Bradford D, et al. A phase I trial of low-dose inhaled carbon monoxide in sepsis-induced ARDS. *JCI Insight* 2018;3:e124039. doi:10.1172/jci.insight.124039
38. Dohl J, Foldi J, Heller J, Gasier HG, Deuster PA, Yu T. Acclimation of C2C12 myoblasts to physiological glucose concentrations for in vitro diabetes research. *Life Sci* 2018;211:238-244.
39. Piantadosi CA. Carbon monoxide, reactive oxygen signaling, and oxidative stress. *Free Radic Biol Med* 2008;45:562-569.
40. Zheng M, Zhang Q, Joe Y, et al. Carbon monoxide-releasing molecules reverse leptin resistance induced by endoplasmic reticulum stress. *Am J Physiol Endocrinol Metab* 2013;304:E780-E788.
41. Hosick PA, Ahmed EK, Gousset MU, Granger JP, Stec DE. Inhalation of carbon monoxide is ineffective as a long-term therapy to reduce obesity in mice fed a high fat diet. *BMC Obes* 2014;1:6. doi:10.1186/2052-9538-1-6
42. Motterlini R, Foresti R. Biological signaling by carbon monoxide and carbon monoxide-releasing molecules. *Am J Physiol Cell Physiol* 2017;312:C302-C313.
43. Hagihara Y, Fukuda S, Goto S, Iida H, Yamazaki M, Moriya H. How many days per week should rats undergo running exercise to increase BMD? *J Bone Miner Metab* 2005;23:289-294.
44. Pecorella SR, Potter JV, Cherry AD, et al. The HO-1/CO system regulates mitochondrial-capillary density relationships in human skeletal muscle. *Am J Physiol Lung Cell Mol Physiol* 2015;309:L857-L871.
45. Tanaka T, Nishimura A, Nishiyama K, Goto T, Numaga-Tomita T, Nishida M. Mitochondrial dynamics in exercise physiology. *Pflugers Arch* 2020;472:137-153. doi:10.1007/s00424-019-02258-3